INTERNATIONAL JOURNAL OF CLIMATOLOGY
Int. J. Climatol. **32**: 2301–2310 (2012)
Published online 15 November 2011 in Wiley Online Library
(wileyonlinelibrary.com) DOI: 10.1002/joc.3400

RMetS
Royal Meteorological Society

Influences of the El Niño Southern Oscillation and the Pacific Decadal Oscillation on the timing of the North American spring

Gregory J. McCabe,[a]*† Toby R. Ault,[b] Benjamin I. Cook,[c]† Julio L. Betancourt[d]† and Mark D. Schwartz[e]

[a] *US Geological Survey, Denver, Colorado, USA*
[b] *Department of Geosciences, University of Arizona, Tucson, Arizona, USA*
[c] *NASA Goddard Institute for Space Studies, New York, New York, USA*
[d] *US Geological Survey, Tucson, Arizona, USA,*
[e] *Department of Geography, University of Wisconsin-Milwaukee, Milwaukee, Wisconsin, USA*

ABSTRACT: Detrended, modelled first leaf dates for 856 sites across North America for the period 1900–2008 are used to examine how the El Niño Southern Oscillation (ENSO) and the Pacific Decadal Oscillation (PDO) separately and together might influence the timing of spring. Although spring (mean March through April) ENSO and PDO signals are apparent in first leaf dates, the signals are not statistically significant (at a 95% confidence level (p <0.05)) for most sites. The most significant ENSO/PDO signal in first leaf dates occurs for El Niño and positive PDO conditions. An analysis of the spatial distributions of first leaf dates for separate and combined ENSO/PDO conditions features a northwest–southeast dipole that is significantly (at p <0.05) different than the distributions for neutral conditions. The nature of the teleconnection between Pacific SST's and first leaf dates is evident in comparable composites for detrended sea level pressure (SLP) in the spring months. During positive ENSO/PDO, there is an anomalous flow of warm air from the southwestern US into the northwestern US and an anomalous northeasterly flow of cold air from polar regions into the eastern and southeastern US. These flow patterns are reversed during negative ENSO/PDO. Although the magnitudes of first leaf date departures are not necessarily significantly related to ENSO and PDO, the spatial patterns of departures are significantly related to ENSO and PDO. These significant relations and the long-lived persistence of SSTs provide a potential tool for forecasting the tendencies for first leaf dates to be early or late. Copyright © 2011 Royal Meteorological Society

KEY WORDS spring; phenology; ENSO; PDO

Received 13 December 2010; Revised 5 October 2011; Accepted 8 October 2011

1. Introduction

The timing of phenological events (seasonal changes in plant and animal activity) are sensitive to climatic variability and change (Running and Hunt, 1993; Myneni *et al*., 1997; Schwartz, 1997, 1998; Menzel and Fabian, 1999; Sparks and Crick, 1999; Schwartz and Reiter, 2000; Cayan *et al*., 2001; Parmesan and Yohe, 2003; Menzel *et al*., 2006; Schwartz *et al*., 2006). Long-term, synoptic phenological observations are rare in North America, but certain phenological traits of select species can be modelled from climate data and then mapped at the continental scale. For example, the Spring Indices 'suite of metrics' (Schwartz and Reiter, 2000) use models of lilac (*Syringa chinensis* 'Red Rothomagensis') and honeysuckle (*Lonicera tatarica* 'Arnold Red', and *L. korolkowii* 'Zabeli'), validated with continental-scale networks of actual phenological observations, as proxies for the occurrence of first leaf, first bloom, and other temperature-sensitive responses to climate. Further, these Spring Indices (SI) provide an effective approach for processing climate data into metrics that are broadly representative of many deciduous plant species in temperate regions, and thus provide a long-term (1900–2008) and spatially widespread dataset of relevant phenoclimatic indicators (Schwartz *et al*., 2006).

Analyses of time series of SI first leaf and first bloom dates for sites across North America have identified regional differences in the variability and long-term trends of these phenological indicators and have indicated long-term trends to an earlier onset of spring associated with warming temperatures, especially for the northwestern US (Schwartz and Reiter, 2000). As might be expected, these trends are evident in monthly averages of springtime temperatures and actual phenological observations made for lilac and honeysuckle since 1956 (Cayan *et al*., 2001). The ultimate causes of interannual variations, secular trends, and their regional differences,

* Correspondence to: G. J. McCabe, US Geological Survey, Denver Federal Center, MS 412, Denver, CO 80225.
E-mail: gmccabe@usgs.gov
† The contributions of these authors to this article were prepared as part of their official duties as United States Federal Government employees.

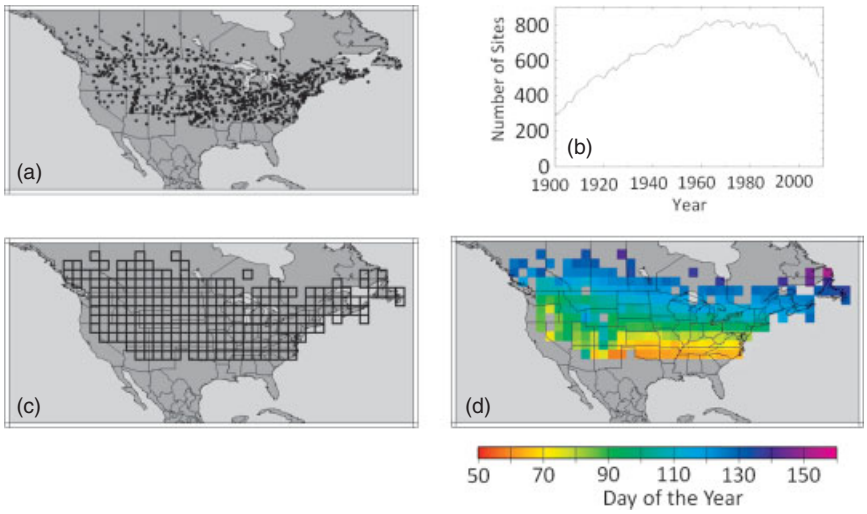

Figure 1. (A) location of modelled first leaf date sites used in the study, (B) number of sites with first leaf dates each year from 1900–2008, (C) 2° grid cells, and (D) mean first leaf date (day-of-the-year with 1 January being day 1) for 2° grid cells for the period 1900–2008.

however, are not well understood, and their predictability in both the near and long term remains unexplored.

Spatiotemporal variability in the timing of spring arises from complex climatic variations that are synthesized in indices of large-scale sea-surface temperature (SST), or atmospheric pressure patterns, in important centres of action and their regional teleconnections. Examples include El Niño-Southern Oscillation (ENSO), the North Atlantic Oscillation (NAO), the Pacific North American (PNA) pattern, the Arctic Oscillation (AO) or Northern Annular Mode (NAM), the Pacific Decadal Oscillation (PDO), and the Atlantic Multidecadal Oscillation (AMO). Because they can summarize complex and sequenced weather and climatic conditions into a single value, phenologists have started to employ these indices in explaining phenophase variations for both plants and animals (Cayan *et al*., 2001; Stenseth *et al*., 2003; Hallet *et al*., 2004; Cook *et al*., 2005; Gordo, 2007; Ault *et al*., 2011). Also, seasonal persistence in these geophysical indices, or lags in their teleconnections, could inform long-lead forecasts of the onset of spring and related phenomena.

The ENSO and the PDO have been identified as important modes of global climate variability that influence the variability of temperature and precipitation for various regions around the world (Kiladis and Diaz, 1989; Mantua and Hare, 2002). There have been many studies of the influences of ENSO and PDO on North American climate (Cayan and Peterson, 1989; Redmond and Koch, 1991; Kahya and Dracup, 1993; Latif and Barnett, 1996; Mantua *et al*., 1997; Gershunov and Barnett, 1998; McCabe and Dettinger, 1999; McCabe and Muller, 2002; McCabe and Wolock, 2008). In addition, several studies have investigated how ENSO and PDO interact and modify the expected ENSO hydroclimatic influences in the US (Gershunov and Barnett, 1998; McCabe and Dettinger, 1999; Gutzler *et al*., 2002; Kurtzman and Scanlon, 2007).

As ENSO and PDO are important modes of the global climate system and have substantial influences on the climate of North America, this study addresses the effects of ENSO and PDO on the onset of spring in North America as represented by modelled first leaf dates. The objectives of this study are to improve understanding of the climate factors that influence the variability of the onset of spring in North America, and to determine the possibility to forecast the onset of spring using ENSO and PDO indices (i.e. spring NINO3.4 SSTs and spring PDO).

2. Methods and data

A dataset of modelled first leaf and first bloom dates has been developed by Schwartz and Reiter (2000) and extended by Schwartz *et al*. (2006). This dataset includes first leaf and first bloom dates for 856 sites (Figure 1(A)) varying in number from 291 sites in 1900 to 829 sites in 1967 (Figure 1(B)). These first leaf dates were computed using a SI model that is calibrated and validated using observations of first leaf and first bloom dates of lilac and honeysuckle. The first leaf dates used in this study are a model-derived indicator of the onset of spring that integrates a variety of springtime climatological variables (Schwartz and Reiter, 2000; Schwartz *et al*., 2006; Ault *et al*., 2011). Details on the development of the SIs are given in Schwartz *et al*. (2006) and Ault *et al*. (2011); also, Table I has a summary of the steps used to compute the SI first leaf dates. Among other things, our particular variant of the SI model considers chill requirements, the amount of winter chilling required by a plant to terminate dormancy and ensure adequate bud break the following spring. This becomes irrelevant in the warm subtropics, so we did not calculate SI for stations south of 34 °N (Figure 1(A)).

The variability in the number of sites with data is a result of the availability of the necessary climate data (e.g. daily maximum and minimum temperature data) for each site. Comparison of the first leaf and first bloom dates (not shown) indicates substantial similarity between the two datasets. We chose first leaf for our analyses

Table I. Summary of how the Spring Indices first leaf date is calculated.

Step 1: Calculate the day-of-the-year (DOY) dates (after 1 October) when 1375, 1250, and 1250 (for the clone lilac *Syringa chinensis* 'Red Rothomagensis', clone honeysuckle *Lonicera tatarica* 'Arnold Red' (HS 'AR'), and clone honeysuckle *L. korolkowii* 'Zabeli' (HS 'ZB'), sub-models respectively) chilling hours (base temperature 7.2 °C) are reached. Average the three DOY dates to produce **Spring Indices Composite Chill Date.**
Step 2: Determine the DOY dates when the following equations are valid (for each sub-model):
Lilac: $1000 = (3.306 \times \text{MDS0}) + (\text{SYNOP} \times 13.878) + (0.201 \times \text{DDE2}) + (0.153 \times \text{DD57})$
HS 'AR': $1000 = (4.266 \times \text{MDS0}) + (\text{SYNOP} \times 20.899) + (0.248 \times \text{DD57})$
HS "ZB": $1000 = (2.802 \times \text{MDS0}) + (\text{SYNOP} \times 21.433) + (0.266 \times \text{DDE2})$
Where:
MDSO = number of days since sub-model chilling satisfaction date
SYNOP = number of high-energy synoptic events that have occurred since sub-model chilling satisfaction date (three-day cumulative degree-hour accumulations higher than 637 degree-hours (base temp. = 0.6 °C))
DD57 = growing degree-hour accumulation (base temp. = 0.6 °C) over the 3 days that were 5–7 days prior to the current date
DDE2 = growing degree-hour accumulation (base temp. = 0.6 °C] over the 3 days that were 0–2 days prior to the current date
Step 3: Adjust the raw DOY dates determined in Step 2 to account for geographical and temporal bias in the number of high-energy synoptic events, using the following equations:
Lilac: Adjusted date = $0.358 - 0.234 \times \text{RAW}$
HS 'AR': Adjusted date = $1.579 - 0.225 \times \text{RAW}$
HS 'ZB': Adjusted date = $-0.204 - 0.109 \times \text{RAW}$
Where:
RAW = raw DOY dates for each sub-model
Step 4: Average the DOY dates from the three sub-models to produce **Spring Indices First Leaf Date**

because it may be most relevant to large-scale ecosystem processes (e.g. vegetation greenup), and it occurs earlier in the year when the teleconnections with ENSO/PDO are strongest.

Currently, there is no one perfect index for the timing of spring that applies at the continental scale. The advantages of the SI are twofold: first, the SI is queued to the start of the growing season, and necessarily means the same thing year after year. That it is tied to lilac and honeysuckle is unimportant; these linkages just provide proof of concept. The SI is analogous to a drought index; a drought index may not be able to characterize a specific tree species' response to moisture anomalies, but the drought index does mean something 'absolute' in terms of local climate variability through time and across space. The second advantage of the SI is that it only responds to the atmosphere; meaning that it is free of local and, thus, noisy biological and ecological effects. This is important because it maximizes the chances of identifying important relations between large-scale modes of climate variability and the index itself; an advantage other plant-based or data-driven indices (such as greenup) might not have.

To provide century-long time series of first leaf dates, missing data for individual sites were filled using a regression approach. For each year, a regression was developed between first leaf dates (the dependent variable) for sites with data and the latitude and longitude for these sites (the independent variables). The regression was then used to estimate first leaf dates for sites with missing data. The distribution of coefficients of determination for the regressions for each year indicated reliable regression models. The coefficients of determination had a median value of 0.70, and a 25th percentile of 0.64 and a 75th percentile of 0.74.

Because the density of modelled first leaf data is higher in eastern North America than in western North America, one additional step was performed to provide a more even spatial distribution of first leaf dates and to increase the smoothness of first leaf date spatial patterns. This step involved gridding the first leaf data for the 856 sites to $2^\circ \times 2^\circ$ grid cells (2° grid cells) (Figure 1(C)). A $2^\circ \times 2^\circ$ grid resolution provides a large enough number of grid cells for robust statistical analysis and allows most of the grid cells to include multiple sites of first leaf data. Grid cells were retained if at least one site was located within a grid cell. This resulted in a set of 2° grid cells numbering 242. Separate principal components analyses (not shown) of (1) the point data and (2) the 2° gridded data provided nearly the exact same results. This result indicates that little or no information regarding first leaf date variability was lost by gridding the data to the 2° grids.

Figure 1(D) illustrates the mean first leaf date for the period 1900–2008. Mean first leaf dates primarily occur during the months of March through May. Because the first leaf dates for most sites occur during the months of March through May, we focused on these months as the period of the analyses (Figure 1(D)). Additionally, the time series of first leaf dates for each 2° grid cell were converted to departures from the respective long-term (1900–2008) mean first leaf dates for each grid cell to make it easier to identify positive and negative departures through time and across space.

Trends in first leaf dates indicate earlier first leaf dates for a large part of the western US and southwestern Canada (Figure 2). These trends to earlier first leaf dates are consistent with increases in spring temperatures in these regions (Cayan *et al*., 2001; Lu *et al*., 2005).

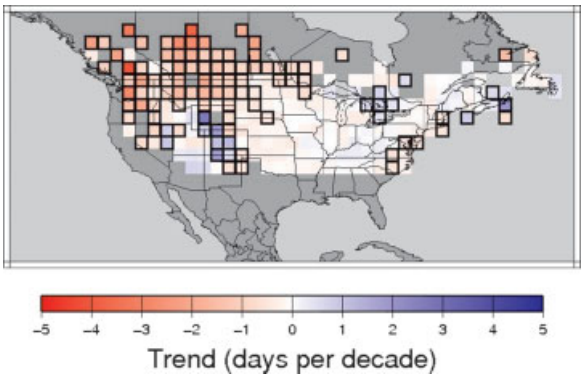

Figure 2. Trends in modelled first leaf dates during the 1900–2008 period. The black squares indicate trends that are statistically significant at $p < 0.05$.

Table II. Number of observations (years) used for neutral MAM NINO3.4 and PDO conditions and separate and combined positive (+) and negative (−) MAM NINO3.4 and MAM PDO conditions.

NINO3.4 and/or PDO Condition	Number of Observations
neutral	16
+NINO3.4	36
−NINO3.4	35
+PDO	36
−PDO	35
+NINO3.4, +PDO	20
−NINO3.4, +PDO	5
+NINO3.4, −PDO	5
−NINO3.4, −PDO	17

Because trends can influence analyses of temporal variability in data time series, the linear trends in the 2° gridded time series of first leaf dates were removed.

NINO3.4 SSTs are a useful index of ENSO (Trenberth, 1997). For this study, monthly NINO3.4 SSTs were computed from the Kaplan monthly SST dataset (http://www.esrl.noaa.gov/psd/data/gridded/data.kaplan_sst.html). Monthly SSTs averaged for the region from 5 °S to 5 °N and from 170 °W to 120 °W were used to represent NINO3.4 SSTs. A time series of monthly PDO values was obtained from http://jisao.washington.edu/pdo. The monthly values of NINO3.4 SSTs and PDO were averaged for the months of March through May (MAM) to generate times series of MAM NINO3.4 SSTs and MAM PDO values for the years 1900–2008. Similar to the first leaf date time series, linear trends in MAM NINO3.4 and MAM PDO time series were removed for the analyses in this study.

The analyses in this study primarily involve computing (and mapping) mean departures (in days) of detrended mean first leaf dates for combinations of positive and negative detrended MAM NINO3.4 and detrended MAM PDO conditions. Positive and negative MAM NINO3.4 and MAM PDO conditions were determined based on terciles computed for the detrended MAM NINO3.4 and detrended MAM PDO time series (1900–2008). Thus, the upper (lower) terciles were used to identify positive (negative) MAM NINO3.4 and MAM PDO conditions. Neutral MAM NINO3.4 and MAM PDO conditions were identified as years when both the NINO3.4 and PDO values were in the middle tercile of the respective distributions. Terciles were used instead of quartiles to allow enough years to be included in each category for statistical analysis.

For each site and sets of years for combinations of positive and negative MAM NINO3.4 and MAM PDO conditions, mean departures (in days) of first leaf dates were computed. The mean departures were subsequently mapped and the maps were examined and compared to identify influences of ENSO and PDO on the variability of first leaf dates. The number of observations (years) used for neutral March through May (MAM) NINO3.4 and PDO conditions and separate and combined positive and negative MAM NINO3.4 and MAM PDO conditions are listed in Table II.

Student's *t*-tests were used to identify mean departures that are significantly different (at a 95% confidence level, $p < 0.05$) from neutral conditions. In addition, statistical tests were performed to determine if the number of statistically significant departures was significantly different from what would be expected (field significance test) (Livezey and Chen, 1983; McCabe and Dettinger, 1999). The determination of whether the number of negative and positive departures was statistically significant (at $p < 0.05$) was accomplished through a Monte Carlo analysis in which 1000 'pseudo-NINO3.4' and 'pseudo-PDO' time series were generated using a stochastic model. The simulated time series were 109 years in length (the same length as the record of first leaf data), and the simulated time series preserved the lag-1 autocorrelations in the NINO3.4 and PDO time series as well as the underlying correlation between NINO3.4 and PDO (Newman *et al.*, 2003).

The 1000 simulated time series of detrended MAM NINO3.4 and PDO were then used to select sets of years to compute mean departures of 2° gridded first leaf dates for each combination of positive/negative MAM NINO3.4 and MAM PDO conditions. For each of the 1000 simulations the numbers of negative and positive significant departures (at $p < 0.05$) were computed. From these values, the 95th percentile values of the number of significant negative and positive departures were computed and used as thresholds of statistical significance (field significance) for the numbers of significant negative and positive departures resulting from the original first leaf data for separate and combined MAM NINO3.4 and MAM PDO conditions.

3. Results and discussion

Figure 3 illustrates mean departures of first leaf dates for positive and negative MAM NINO3.4 SSTs and positive and negative MAM PDO. For these composites, NINO3.4 and PDO effects are considered separately. Given that

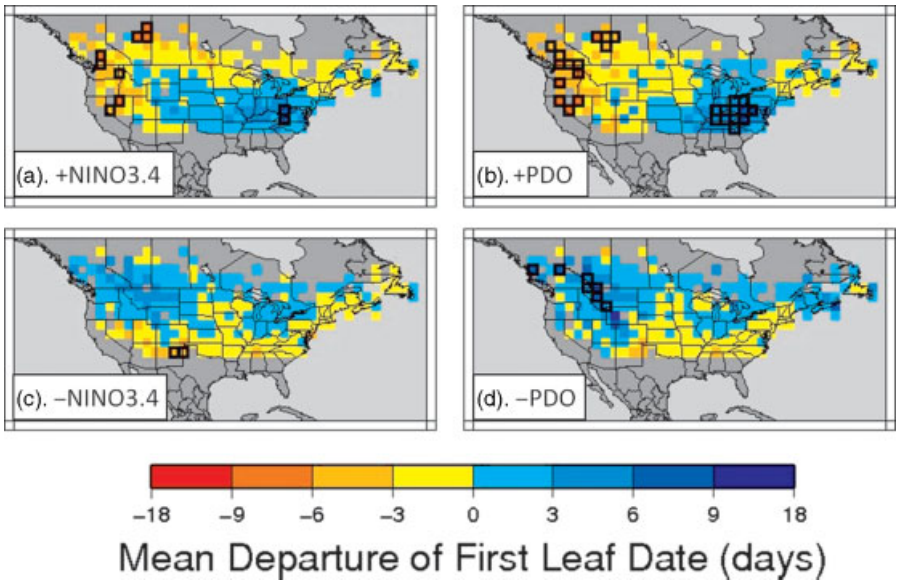

Figure 3. Mean departure of modelled first leaf date for positive (+) and negative (−) MAM NINO3.4 SSTs and MAM PDO during 1900–2008. The black squares indicate departures that are statistically significant at $p < 0.05$.

MAM NINO3.4 and MAM PDO are related SST indices, the spatial patterns of mean departures of first leaf dates are expectedly similar for both SST indices. For positive MAM NINO3.4 (Figure 3(A)) and positive MAM PDO (Figure 3(B)), departures of first leaf dates are negative (earlier first leaf dates) in the northwestern US and southwestern Canada and are positive (later first leaf dates) in the southeastern US. For negative MAM NINO3.4 (Figure 3(C)) and negative MAM PDO (Figure 3(D)), departures of first leaf dates are positive in the northwestern US and southwestern Canada and negative in the southeastern US. These patterns of departures of first leaf dates are consistent with patterns of temperature anomalies in North America associated with NINO3.4 and PDO (Kiladis and Diaz, 1989; Redmond and Koch, 1991; Mantua and Hare, 2002). When NINO3.4 and PDO are positive (negative), positive (negative) temperature anomalies occur in the northwestern US and, consequently, negative (positive) temperature anomalies occur in the southeastern US.

For positive MAM PDO (Figure 3(B)) the mean departures of first leaf dates are significantly ($p < 0.05$) different from neutral conditions for a number of grid cells, whereas there are only a few grid cells with significant departures for positive and negative MAM NINO3.4 (Figures 3(A) and (C)), and negative MAM PDO (Figure 3(D)). An analysis of the number of grid cells with statistically significant (at $p < 0.05$) differences from neutral conditions indicates that the number of significant differences for none of the composite maps exceed the expected value (determined using a field significance test and a significance level of $p < 0.05$).

Gershunov and Barnett (1998) suggest that when NINO3.4 SSTs and PDO are in similar phases that the effects of these SST patterns on North American climate are amplified (i.e. constructive phases). To examine these effects, mean departures of first leaf dates for combinations of positive/negative MAM NINO3.4 and positive/negative MAM PDO were computed.

For combined positive MAM NINO3.4 and positive MAM PDO conditions, the mean departures of first leaf dates are negative (earlier first leaf dates) in the northwestern US and southwestern Canada (Figure 4(A)). Positive departures (later first leaf dates) primarily occur in the southeastern US. This spatial pattern of first leaf date departures is consistent with the effects of El Niño (and positive PDO) conditions on temperatures across North America (Redmond and Koch, 1991; Mantua and Hare; 2002). During El Niño (and positive PDO) temperatures in the northwestern US and southwestern Canada are generally warmer than average (resulting in earlier first leaf dates), and temperatures in the southeastern US are generally cooler than average (resulting in later first leaf dates) (Redmond and Koch, 1991; Mantua and Hare, 2002).

In contrast, during combined negative MAM NINO3.4 and negative MAM PDO conditions, the spatial pattern of first leaf date departures indicates positive departures in the northwestern US (and southwestern Canada) and negative in the southeastern US (Figure 4(D)). This pattern of departures of first leaf dates is negatively correlated with the pattern for combined positive MAM NINO3.4 and positive MAM PDO (Pearson correlation coefficient $(r) = -0.32$, $p < 0.01$).

For combined positive MAM NINO3.4 and negative MAM PDO conditions (Figure 4(C)), the spatial pattern of first leaf departures indicates a mixture of departures; whereas, for combined negative MAM NINO3.4 and positive MAM PDO (Figure 4(B)), the first leaf departures are negative for most of the western US and southwestern Canada, and positive for most of the eastern US.

The pattern of first leaf departures for combined positive MAM NINO3.4 and positive MAM PDO (Figure 4(A)) appears to be the strongest of the patterns

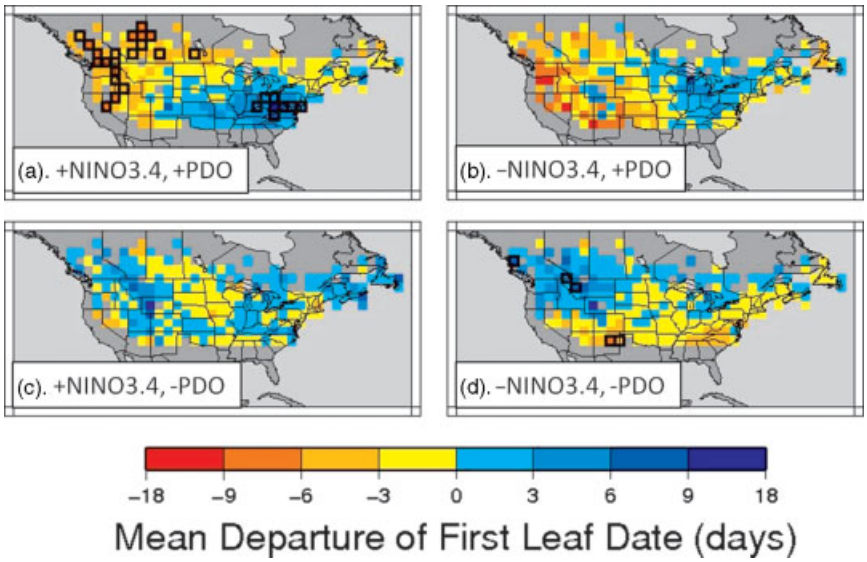

Figure 4. Mean departure of modelled first leaf date (in days) for combinations of positive (+) and negative (−) MAM NINO3.4 SSTs and MAM PDO during 1900–2008. The black squares indicate departures that are statistically significant at $p < 0.05$.

of combined positive MAM NINO3.4 and negative MAM PDO conditions, with 20 grid cells indicating significant negative departures and 7 grid cells with significant positive departures. However, these numbers of significant positive and negative departures is less than the expected number for the number of grid cells, using a 95% confidence level.

3.1. Differences across space

Although the mean departures of first leaf dates did not indicate many statistically significant departures (at $p < 0.05$) for separate and combined MAM NINO3.4 and MAM PDO conditions, the effects of NINO3.4 and PDO could be seen in the patterns of departures and these patterns are consistent with the effects of NINO3.4 and PDO on North American temperature (Redmond and Koch, 1991; Mantua and Hare, 2002). The effects of NINO3.4 and PDO on first leaf date departures also can be seen in the frequency distributions of first leaf date departures for separate and combined MAM NINO3.4 and MAM PDO conditions. Figure 5 illustrates frequency distributions of first leaf date departures (expressed as probability density functions (pdfs)) for separate and combined MAM NINO3.4 and MAM PDO conditions). The pdfs of first leaf date departures for NINO3.4 and PDO conditions are flatter and wider than is the pdf for neutral conditions. Flatter and wider pdfs indicate fewer values near the centre of the range of values, and more values toward the tails of the distribution. The flatter and wider pdfs for NINO3.4 and PDO conditions, compared with the pdf for neutral conditions, suggests an effect of NINO3.4 and PDO on first leaf date departures. Additionally, the pdfs for positive NINO3.4 and positive PDO (Figure 5(A)) are flatter and wider than are the pdfs for negative NINO3.4 and negative PDO. For combinations of NINO3.4 and PDO the pdfs for positive NINO3.4 and positive PDO, and negative NINO3.4 and positive PDO are flatter and wider than any of the pdfs for other combined effects (Figure 5(B)). These results suggest that positive PDO conditions have a stronger effect on first leaf departures than does NINO3.4.

The Index of Agreement (d) was used to compare the distributions of first leaf date departures for separate and combined MAM NINO3.4 and MAM PDO conditions with the distribution of first leaf date departures for neutral conditions (Willmott, 1981, 1984; Legates and McCabe, 1999). The Index of Agreement is often used to compare two time series (e.g. measured and modelled time series), but it also can be used to compare samples of paired data. For our application, d is computed as

$$d = 1. - \frac{\sum_{i=1}^{N}(S1_i - S2_i)^2}{\sum_{i=1}^{N}(|S2_i - \overline{S1}| - |S1_i - \overline{S1}|)^2} \qquad (1)$$

where N is the number of sites, $S1_i$ is the sample 1 value for site i, $S2_i$ is the sample 2 value for site i, and $\overline{S1}$ is the mean for all sites in sample 1. The Index of Agreement ranges from 0 to 1, with a value of 1 indicating perfect agreement between two samples. The Index of Agreement represents an improvement over the coefficient of determination (r^2) for sample comparisons because it is sensitive to differences in both means and variances of two samples (Legates and McCabe, 1999).

The d statistics for all of the comparisons of the first leaf date distributions for separate and combined NINO3.4 and PDO conditions with the distribution for neutral NINO3.4 and PDO are near zero (Table III). These results indicate that the first leaf date distributions for separate and combined NINO3.4 and PDO conditions are substantially different from the distribution for neutral conditions. These results indicate that the effects of NINO3.4 and PDO are

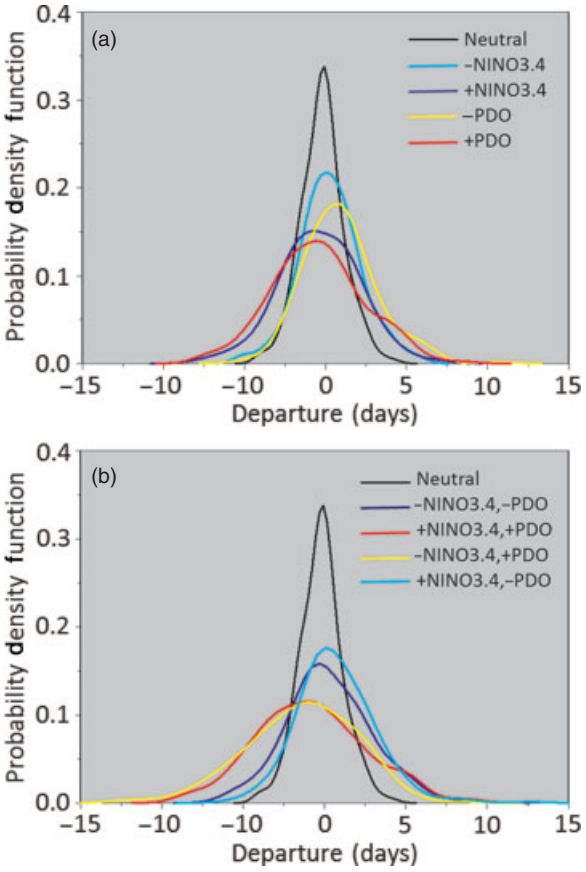

Figure 5. Probability density functions of the distributions of mean departures of modelled first leaf dates for (A) positive (+) and negative (−) MAM NINO3.4 SSTs (NINO3.4) and MAM PDO, and (B) combinations of positive and negative MAM NINO3.4 and MAM PDO. The probability density function of mean first leaf date departures for neutral MAM NINO3.4 and MAM PDO conditions is plotted (black line) as a reference for the other distributions.

Table III. Index of Agreement (d) for comparisons of distributions of mean first leaf date departures for separate and combined positive (+) and negative (−) MAM NINO3.4 and MAM PDO conditions with the distribution of mean first leaf date departures for neutral MAM NINO3.4 and MAM PDO conditions.

	d
+NINO3.4	0.03
−NINO3.4	0.09
+PDO	0.06
−PDO	0.10
+NINO3.4, +PDO	0.08
−NINO3.4, +PDO	0.09
+NINO3.4, −PDO	0.13
−NINO3.4, −PDO	0.14

strongly manifested in the spatial patterns of first leaf dates.

3.2. Relations with atmospheric circulation

An examination of sea level pressure (SLP) anomalies for the years included in each of the composites for positive (negative) MAM NINO3.4 and positive (negative) MAM PDO help explain the patterns of the first leaf departures (Figure 6). As with other datasets, the SLP anomalies were detrended before analyses were performed. Since the patterns of mean first leaf departures for the constructive combinations of MAM NINO3.4 and MAM PDO conditions (i.e. positive NINO3.4 and positive PDO, and negative NINO3.4 and negative PDO) included the largest number of observations and indicated the strongest effects of NINO3.4 and PDO on first leaf dates, SLP anomalies for these two conditions are examined (Figure 6).

For combined positive MAM NINO3.4 and positive MAM PDO conditions (Figure 6(A)), positive SLP anomalies are centred over central Canada and the north-central US; whereas, negative SLP anomalies occur over the eastern North Pacific Ocean and extend into western North America (i.e. a strengthened Aleutian Low). Negative SLP anomalies also occur over the western North Atlantic Ocean and extend into the southeastern US. These SLP anomalies suggest an anomalous flow of warm air from the southwestern US into the northwestern US and an anomalous northeasterly flow of cold air from polar regions into the eastern and southeastern US. These SLP anomalies and the associated anomalous flows of air are consistent with warmer-than-average spring temperatures (early first leaf dates) in the northwestern US and southwestern Canada, and cooler-than-average spring temperatures (late first leaf dates) in the southeastern US.

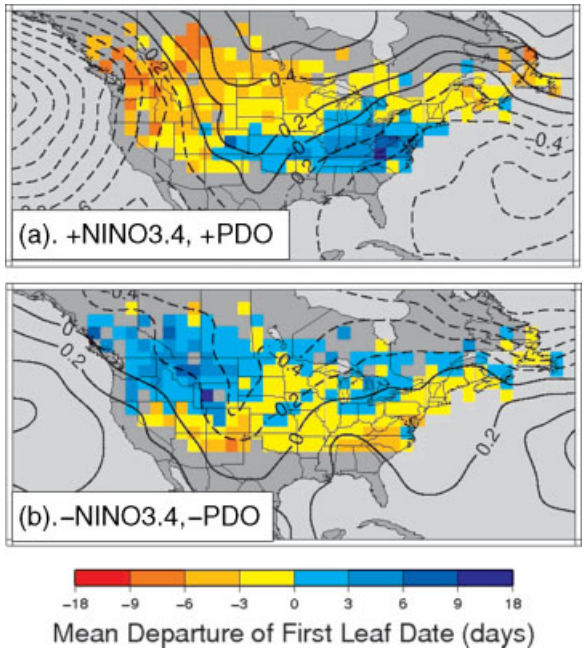

Figure 6. Mean departure of modelled first leaf date (in days) for (A) positive MAM NINO3.4 SSTs and positive MAM PDO, and (B) negative MAM NINO3.4 SSTs and negative MAM PDO, during 1900–2008, and associated SLP anomalies (in hectoPascals). The solid lines indicate positive SLP anomalies and dashed lines indicate negative SLP anomalies. The contour interval is 0.2 hectoPascals.

In contrast, for combined negative MAM NINO3.4 and negative MAM PDO conditions (Figure 6(B)) negative SLP anomalies occur over Canada and the north-central US and positive SLP anomalies occur over the North Pacific and North Atlantic Oceans. This pattern of SLP anomalies is the opposite of the pattern of SLP anomalies for positive NINO3.4 and positive PDO conditions ($r = -0.68$, $p < 0.01$). These SLP anomalies indicate an anomalous northwesterly flow of cool air (and late first leaf departures) into southwestern Canada and the northwestern US, and an anomalous southwesterly flow of warm air (resulting in negative first leaf departures) into the southeastern US.

The first leaf date departures in western North America and the associated SLP anomalies for positive NINO3.4 and PDO (Figure 6(A)) conditions and negative NINO3.4 and PDO conditions (Figure 6(B)) are consistent with results for ENSO and PDO relations with ice duration on lakes and rivers in Canada given by Bonsal *et al*., 2006, who found that ENSO and PDO had substantial effects on ice duration. They found that positive phases of ENSO and PDO are associated with shorter ice durations consisting of later freeze-ups and earlier break-ups. In contrast, negative phases of ENSO and PDO were associated with longer ice duration over much of Canada. These results are consistent with previous analyses that showed that positive ENSO and PDO conditions are associated with warmer temperatures over much of Canada, particularly in western Canada during winter and spring (e.g. Bonsal *et al*., 2001). Bonsal *et al*. (2006) suggest that the higher temperatures over western Canada and resultant shorter ice durations during positive ENSO and PDO conditions are mainly attributable to a strengthened Aleutian Low and associated warm air advection into much of Canada (Figure 6(A)).

The analysis of SLP anomalies associated with the spatial patterns of first leaf date departures indicates that ENSO and PDO variability influence the timing of first leaf in North America through effects of SLP patterns on temperature.These analyses provide a physical explanation for the variability of departures of first leaf dates for combinations of NINO3.4 and PDO conditions. In addition, although the magnitudes of first leaf departures are not strongly related to NINO3.4 and PDO variability, the spatial patterns of first leaf dates and the tendencies to be early or late are substantially related to NINO3.4 and PDO.

3.3. Potential for forecasts of first leaf date departures

The relations between first leaf dates and NINO3.4 and PDO, and the persistence of SSTs (Table IV) suggest potential for forecasts of the tendency of first leaf dates to be early or late. The relations of NINO3.4 and PDO with SLP anomalies (Figure 6) also suggest the possibility of using SLPs to forecast the tendency for early or late first leaf dates. However, the atmosphere does not have as much persistence as do SSTs. For example, the PNA index characterizes large-scale atmospheric circulation over North America (Wallace and Gutzler, 1981; Yarnal and Diaz, 1986; Yarnal and Leathers, 1988) and has been recognized as a primary mode of atmospheric circulation variability over North America (Barnston and Livezey, 1987; Leathers and Palecki, 1992). The PNA serves as a measure of the relative amplitude of the stationary waves over North America and has proven to be useful to understand climate variability over on time scales ranging from months to decades (Leathers and Palecki, 1992). Additionally, the PNA is related to variability in NINO3.4 and PDO (Yu and Zwiers, 2007).

Table IV. Correlations of mean three-month average NINO3.4 SSTs, PDO, and the PNA index with mean average MAM values.

	NINO3.4	PDO	PNA
OND	0.75	0.57	0.01
NDJ	0.77	0.64	0.03
DJF	0.80	0.76	0.03
JFM	0.84	0.87	0.59
FMA	0.87	0.96	0.81
MAM	1.00	1.00	1.00

Correlations between MAM PNA and the PNA averaged for three-month periods before the spring season show that the persistence of PNA is short-lived (Table IV), whereas the persistence of NINO3.4 and PDO is large and long-lived. Thus, SSTs likely provide the best opportunity for potential forecasts of first leaf dates.

To explore the potential for forecasting first leaf date departures, time series of average NINO3.4 and PDO for the OND period were used to compute the risk of early first leaf dates. Risks were computed for the constructive combinations of NINO3.4 and PDO (i.e. positive NINO3.4 and positive PDO conditions, and negative NINO3.4 and negative PDO conditions). There are 18 years during 1900–2008 with positive OND NINO3.4 and positive OND PDO conditions, and 19 years with negative OND NINO3.4 and negative OND PDO conditions. Risk of early first leaf dates was computed as the number of years indicating first leaf dates in the lowest percentile during 1900–2008 at each 2° grid cell (expressed as a percentage of the total number of years for the constructive combinations of OND NINO3.4 and OND PDO). These results suggest that there may be potential to forecast at least the spatial pattern of first leaf date departures when NINO3.4 SSTs and PDO are in positive phases.

Results indicate that for positive OND NINO3.4 and positive OND PDO conditions the risk of early first leaf dates is greater than 50% for much of the northwestern US and southwestern Canada (Figure 7(A)). For these NINO3.4 and PDO conditions, the risk of early first leaf dates is lowest (less than 10%) in the southeastern US. This pattern of risks of early first leaf dates suggests that useful forecasts of early first leaf dates may be possible

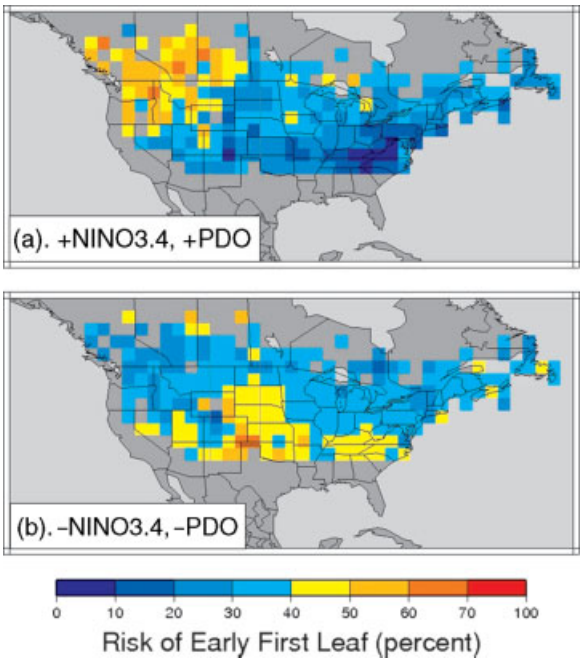

Figure 7. Risk of early modelled first leaf date for (A) positive OND NINO3.4 and positive OND PDO conditions, and (B) negative OND NINO3.4 and negative OND PDO conditions during 1900–2008.

for several months ahead of the spring season when positive NINO3.4 and positive PDO conditions exist.

For negative OND NINO3.4 and negative OND PDO conditions the pattern of risks of first leaf dates indicates low risks for most locations across the northern US and southern Canada, and higher risks across the southern US (Figure 7(B)). The highest risks of early first leaf dates for these conditions are not as high as the highest risks indicated for positive OND NINO3.4 and positive OND PDO conditions (Figure 7(A)). This result is not surprising given that the persistence of negative NINO3.4 and negative PDO conditions does not appear to be as strong as is the persistence of positive NINO3.4 and positive PDO conditions. Thus, the forecasts using negative NINO3.4 and negative PDO conditions likely are less reliable than those made using positive NINO3.4 and positive PDO conditions.

4. Conclusions

Time series of SI first leaf dates, an index of the onset of spring, for 856 sites across North America for the period 1900–2008 were analysed to examine the effects of ENSO and PDO variability on the timing of spring. Results indicate noticeable (although not necessarily statistically significant) temporal effects of ENSO and PDO on the timing of first leaf dates in the northwestern US and southwestern Canada. During El Niño and positive PDO conditions, first leaf dates are generally earlier in the northwestern US and later in the eastern US. With La Niña and negative PDO conditions, the opposite pattern of first leaf date departures generally occurs.

Although the temporal effects of ENSO and PDO on first leaf dates is not necessarily statistically significant, analyses of differences in the spatial patterns of first leaf dates associated with ENSO and PDO indicate highly statistically significant differences from neutral conditions for all separate and combined conditions of NINO3.4 and PDO. In addition, the spatial patterns of first leaf date departures can be explained by differences in SLP anomalies driven by NINO3.4 and PDO. Results also suggest that the persistence of NINO3.4 and PDO when in positive phases may be useful to forecast spatial patterns of first leaf date departures.

Acknowledgements

This work was conducted as a part of the 'Forecasting Phenology: Integrating Ecology, Climatology, and Phylogeny to Understand Plant Responses to Climate Change' Working Group supported by the National Center for Ecological Analysis and Synthesis, which is funded by NSF (Grant #EF-0553768), the University of California, Santa Barbara, and the State of California. Additional support was also provided by the USA-National Phenology Network, supported by a Research Coordination Network grant from the National Science Foundation (NSF Grant IOS-0639794).

References

Ault TR, Macalady AK, Pederson GT, Betancourt JL, Schwartz MD. 2011. Northern Hemisphere modes of variability and the timing of spring in western North America. *Journal of Climate*. DOI: 10.1175/2011JCLI4069.1.

Barnston AG, Livezey RE. 1987. Classification, seasonality and persistence of low-frequency atmospheric circulation patterns. *Monthly Weather Review* **115**: 1083–1126.

Bonsal BR, Prowse TD, Duguay CR, Lacrois MP. 2006. Impacts of large-scale teleconnections on freshwater-ice break/freeze-up dates over Canada. *Journal of Hydrology* **330**: 340–353.

Bonsal BR, Shabbar A, Higuchi K. 2001. Impacts of low frequency variability modes on Canadian winter temperature. *International Journal of Climatology* **21**: 95–108.

Cayan DR, Kammerdiener SA, Dettinger MD, Caprio JM, Peterson DH. 2001. Changes in the onset of spring in the western US. *Bulletin of the American Meteorological Society* **82**: 399–415.

Cayan DR, Peterson DH. 1989. The influence of North Pacific atmospheric circulation on streamflow in the west. In *Aspects of Climate Variability in the Pacific and Western Americas,* Peterson DH (ed). *Geophysical Monograph*, No. 55, American Geophysical Union: Washington, DC. 375–397.

Cook BI, Smith TS, Mann MA. 2005. The North Atlantic Oscillation and regional phenology prediction over Europe. *Global Change Biology* **11**: 919–926.

Gershunov A, Barnett TP. 1998. Interdecadal modulation of ENSO teleconnections. *Bulletin of the American Meteorological Society* **79**: 2715–2725.

Gordo O. 2007. Why are bird migration dates shifting? A review of weather and climate effects on avian migratory phenology. *Climate Research* **35**: 37–58.

Gutzler DS, Kann DM, Thornbrugh C. 2002. Modulation of ENSO-based long-lead outlooks of Southwestern U.S. winter precipitation by the Pacific Decadal Oscillation. *Weather Forecasting* **17**: 1163–1172.

Hallett TB, Coulson T, Pilkington JG, Clutton-Brock TH, Pemberton JM, Grenfell BT. 2004. Why large-scale climate indices seem to predict ecological processes better than local weather. *Nature* **430**: 71–75.

Kahya E, Dracup JA. 1993. U.S. streamflow patterns in relation to the El Nino/Southern Oscillation. *Water Resources Research* **29**: 2491–2503.

Kiladis GN, Diaz HF. 1989. Global climatic anomalies associated with extremes of the Southern Oscillation. *Journal of Climate* **2**: 1029–1090.

Kurtzman D, Scanlon BR. 2007. El Niño–Southern Oscillation and Pacific Decadal Oscillation impacts on precipitation in the southern and central United States: Evaluation of spatial distribution and predictions. *Water Resources Research* **43**: W10427, DOI: 10.1029/2007WR005863.

Latif M, Barnett TP. 1996. Decadal climate variability over the North Pacific and North America: Dynamics and predictability. *Journal of Climate* **9**: 2407–2423.

Leathers DJ, Palecki MA. 1992. The Pacific/North American teleconnection pattern and the United States climate. Part 11. Temporal characteristics and index specification. *Journal of Climate* **5**: 707–716.

Legates DR, McCabe GJ. 1999. Evaluating the use of "goodness-of-fit" measures in hydrologic and hydroclimatic model validation. *Water Resources Research* **35**: 233–241.

Livezey RE, Chen W. 1983. Statistical field significance and its determination by Monte Carlo methods. *Monthly Weather Review* **111**: 46–59.

Lu QQ, Lund R, Seymour L. 2005. An update on U.S. temperature trends. *Journal of Climate* **18**: 4906–4914.

Mantua NJ, Hare SR. 2002. The Pacific Decadal Oscillation. *Journal of Oceanography* **58**: 35–44.

Mantua NJ, Hare SR, Zhang Y, Wallace JM, Francis RC. 1997. A Pacific interdecadal climate oscillation with impacts on salmon production. *Bulletin of the American Meteorological Society* **78**: 1069–1079.

McCabe GJ, Dettinger MD. 1999. Decadal variations in the strength of ENSO teleconnections with precipitation in the western United States. *International Journal of Climatology* **19**: 1399–1410.

McCabe GJ, Muller RA. 2002. Effects of ENSO on weather-type frequencies and properties at New Orleans, Louisiana. *Climate Research* **20**: 95–105.

McCabe GJ, Wolock DM. 2008. Joint variability of global runoff and global sea-surface temperatures. *Journal of Hydrometeorology* **9**: 816–824.

Menzel A, Fabian P. 1999. Growing season extended in Europe. *Nature* **397**: 659.

Menzel A, Sparks TH, Estrella N, Koch E, Aasa A, Ahas R, Alm-Kübler K, Bissolli P, Braslavska O, Briede A, Chmielewski FM, Crepinsek Z, Curnel Y, Dahl Å, Defila C, Donnelly A, Filella Y, Jatczak K, Måge F, Mestre A, Nordli Ø, Peñuelas J, Pirinen P, Remišová V, Scheifinger H, Striz M, Susnik A, van Vliet AJ, Wielgolaski F-E, Zach S, Zust A. 2006. European phenological response to climate change matches the warming pattern. *Global Change Biology* **12**: 1–8.

Myneni RB, Keeling CD, Tucker CJ, Asrar G, Nemani RR. 1997. Increased plant growth in the northern high latitudes from 1981–1991. *Nature* **386**: 698–702.

Newman M, Compo GP, Alexander MA. 2003. ENSO-forced variability of the Pacific decadal oscillation. *Journal of Climate* **16**: 3853–3857.

Parmesan C, Yohe G. 2003. A globally coherent fingerprint of climate change impacts in natural systems. *Nature* **421**: 37–42.

Redmond KT, Koch RW. 1991. Surface climate and streamflow variability in the western United States and their relationship to large scale circulation indices. *Water Resources Research* **27**: 2381–2399.

Running SW, Hunt ER. 1993. Generalization of a forest ecosystem process model for other biomes, BIOME–BGC and an application for global scale models. In *Scaling Physiological Processes, Leaf to Globe*, Field C, Ehleringer J (eds). Academic Press: New York, 144–157.

Schwartz MD. 1997. Spring index models: an approach to connecting satellite and surface phenology. In *Phenology of Seasonal Climates*, Lieth H, Schwartz MD (eds). Backhuys: The Netherlands, 23–38.

Schwartz MD. 1998. Green-wave phenology. *Nature* **394**: 839–840.

Schwartz MD, Ahas R, Aasa A. 2006. Onset of spring starting earlier across the Northern Hemisphere. *Global Change Biology* **12**: 343–351.

Sparks T, Crick H. 1999. The times are a-changing? *Bird Conservation International* **9**: 1–7.

Schwartz MD, Reiter BE. 2000. Changes in North American spring. *International Journal of Climatology* **20**: 929–932.

Stenseth N, Ottersen G, Hurrell J, Mysterud A, Lima M, Chan K, Yoccoz N, Adlandsvik B. 2003. Studying climate effects on ecology through the use of climate indices: the North Atlantic Oscillation, El Nino Southern Oscillation and beyond. *Proceedings of the Royal Society of Biology* **270**: 2087–2096.

Trenberth KE. 1997. The definition of El Nino. *Bulletin of the American Meteorological Society* **78**: 2771–2777.

Wallace JM, Gutzler DS. 1981. Teleconnections in the 500 mb geopotential height field during the Northern Hemisphere winter. *Monthly Weather Review* **109**: 784–812.

Willmott CJ. 1981. On the validation of models. *Physical Geography* **2**: 184–194.

Willmott CJ. 1984. On the evaluation of model performance in physical geography. In *Spatial Statistics and Models*, Gaile GL, Wilmott CJ, Reidel D (eds). Norwell: Massachusetts, 443–460.

Yarnal B, Diaz HF. 1986. Relationships between extremes of the Southern Oscillation and the winter climate of the Anglo-American Pacific coast. *Journal of Climatology* **6**: 197–219.

Yarnal B, Leathers DJ. 1988. Relationships between interdecadal and interannual climatic variations and their effect on Pennsylvania climate. *Annals of the Association of American Geographers* **78**: 624–641.

Yu B, Zwiers FW. 2007. The impact of combined ENSO and PDO on the PNA climate: a 1,000-year climate modeling study. *Climate Dynamics* **29**: 837–851.

